IEEE Access
Multidisciplinary | Rapid Review | Open Access Journal

Received June 17, 2020, accepted June 27, 2020, date of publication July 1, 2020, date of current version July 15, 2020.

Digital Object Identifier 10.1109/ACCESS.2020.3006243

Wideband Filtering Dumbbell-Shaped Slot Antenna With Improved Frequency Selectivity for Both Band-Edges

NA NIE AND ZHI-HONG TU, (Member, IEEE)
School of Electronic and Information Engineering, South China University of Technology, Guangzhou 510641, China
Corresponding author: Zhi-Hong Tu (zhtu@scut.edu.cn)

This work was supported in part by the National Natural Science Foundation of China under Grant 61471172, in part by the Guangzhou Science Technology Project under Grant 201707010360, and in part by the Joint Fund of Shanghai Jiaotong University and Xidian University—the Key Laboratory of Ministry of Education of China for Research of Design and EMC of High Speed Electronic Systems.

ABSTRACT A novel wideband filtering dumbbell-shaped slot antenna with improved frequency selectivity for both band-edges is proposed in this paper. The filtering slot antenna is composed of a dumbbell-shaped slot, two parasitic patches, eight slot-stubs and a feeding line with a pair of step impedance resonator (SIR) stubs. An additional resonance is generated to increase the bandwidth and a gain null is produced at the upper band-edge to improve the frequency selectivity by loading parasitic patches in the dumbbell-shaped slot. Eight slot-stubs adjacent to the dumbbell-shaped slot are etched to enhance the impedance matching. In addition, the bandwidth is further broadened and two gain nulls are realized at both band-edges by adding a pair of SIR stubs. Moreover, the gain nulls can be adjusted individually by the length of parasitic patches or SIR stubs. As a result, the gain curve of the proposed filtering slot antenna has good flatness and the frequency selectivity for both band-edges is significantly improved. A prototype has been manufactured and measured to verify the validity of the design. The measured impedance bandwidth of $|S_{11}| < -10$ dB is 62.5% (2.2 GHz - 4.2 GHz). High suppression levels of 26 dB and 30 dB can be achieved in the lower and upper stopbands, respectively.

INDEX TERMS Filtering slot antenna, wideband, gain nulls, frequency selectivity.

I. INTRODUCTION

Higher requirements for the RF front-end devices are put forward by the communication system, like multi-function and integration. Antennas and filters are two kinds of important front-end devices. Traditionally, antennas and filters have been designed separately, and installing these two devices requires a lot of space. To solve this problem and realize the integration, a variety of antennas with filtering performance have been reported. For the integrated filtering antenna designs in [1]–[7], the radiator acts as the last resonator of the narrow-band filtering circuit, which complicates the antenna structure. Meanwhile, adding complex filtering circuits can result in extra insertion loss and degrade the gain. Though the structures of filtering antennas in [8]–[11] are simple, they suffer limited impedance bandwidths. In order to meet the requirement of high-speed data transmission, it is of great importance to design antennas with wideband performance. Parasitic elements are introduced to widen the bandwidth and achieve the filtering response in [12]–[14]. Broadband filtering antennas with dielectric resonators [15], [16], and metasurface [17], [18] are published. A 3-D integrated filtering magneto-electric dipole antenna is obtained in [19] by etching a pair of C-slots on the planar dipole. However, the profiles of these antennas are high due to the stacked structures.

It is generally known that slot antennas have been widely studied because of their advantages of low profile, easy integration and easy fabrication. In order to increase the operating bandwidth of slot antennas, off-centered microstrip-fed is employed in [20], [21] and multi-mode radiator structure is utilized in [22]. Although the impedance bandwidth is greatly improved, none of them has filtering performance. Recently, broadband filtering slot antennas are put forward in [23], [24], but the frequency selectivity in the gain curve is not good.

The associate editor coordinating the review of this manuscript and approving it for publication was Cesar Vargas-Rosales.

In this work, a wideband filtering dumbbell-shaped slot antenna based on single-layer substrate is proposed. For the design in [25], the dumbbell-shaped slot can be excited by the microstrip line. By loading parasitic patches and step impedance resonator (SIR) stubs, not only the bandwidth of the proposed antenna is significantly broadened, but also three gain nulls in the frequency-dependent gain curve are obtained. Therefore, the selectivity of the proposed antenna is greatly enhanced. Further, the locations of the gain nulls at the lower and upper band can be controlled separately. The proposed antenna has the characteristics of simple structure, wide bandwidth, high out-of-band suppression and improved frequency selectivity.

II. ANTENNA DESIGN

A. ANTENNA STRUCTURE

The geometry of this proposed filtering slot antenna is shown in Fig. 1. The proposed antenna is based on one-layer substrate with the dielectric constant of 4.4, loss tangent of 0.02, and height of 0.8 mm. It consists of a feeding line with SIR stubs, a dumbbell-shaped slot with eight slot-stubs, and two parasitic patches. The feeding line with SIR stubs is on the top of the substrate, and the dumbbell-shaped slot with eight slot-stubs is etched in the ground on the bottom of the substrate. A circle of radius r is added at the ends of the feeding line for improving the impedance matching. Two parasitic patches with width of w_2 and length of l_2 are symmetrically introduced in the dumbbell-shaped slot. The eight slot-stubs have the same width of w_3 and the same length of l_3. A pair of SIR stubs are loaded on both sides of the feeding line. The proposed filtering antenna is only implemented on a single-layer substrate, which achieves the low profile and reduces the manufacturing difficulty. In Fig. 1, the optimized parameter values are shown in detail.

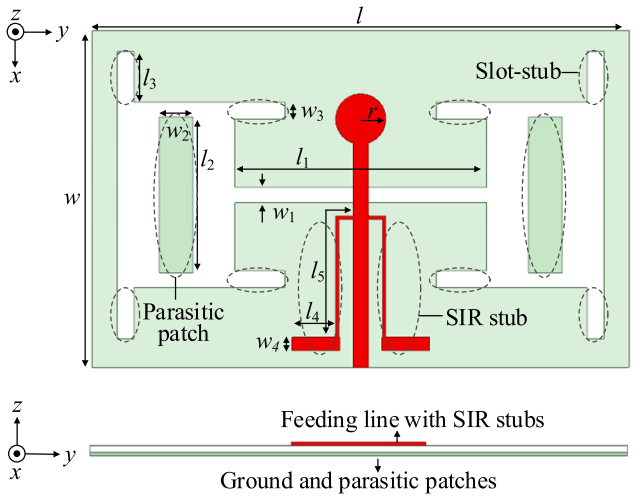

FIGURE 1. Configuration of the proposed filtering dumbbell-shaped slot antenna. (l = 64 mm, w = 40 mm, l_1 = 30 mm, w_1 = 1.8 mm, l_2 = 18.5 mm, w_2 = 4 mm, l_3 = 6 mm, w_3 = 2 mm, l_4 = 5.7 mm, w_4 = 1.6 mm, l_5 = 15.5 mm, r = 3 mm).

B. ANTENNA ANALYSIS

To better illustrate the operating performance of the proposed antenna, the developments of reference antennas from Antenna I to Antenna III are presented in Fig. 2, where the reference and proposed antennas have the same ground size. Fig. 3 and Fig. 4 depict the reflection coefficients and realized gains of the above antennas, respectively. First, Antenna I is the traditional dumbbell-shaped slot antenna which consists of a microstrip feeding line and a dumbbell-shaped slot. It can be found from Fig. 3 that it has only one resonant frequency with narrow impedance bandwidth of 18.1% (2.77 GHz - 3.32 GHz). As seen in Fig. 4, the gain of

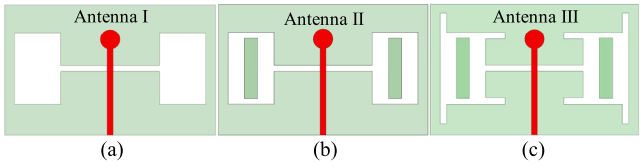

FIGURE 2. Configurations of the reference antennas. (a) Reference Antenna I: conventional dumbbell-shaped slot antenna. (b) Reference Antenna II: dumbbell-shaped slot antenna with parasitic patches. (c) Reference Antenna III: dumbbell-shaped slot antenna with parasitic patches and slot-stubs.

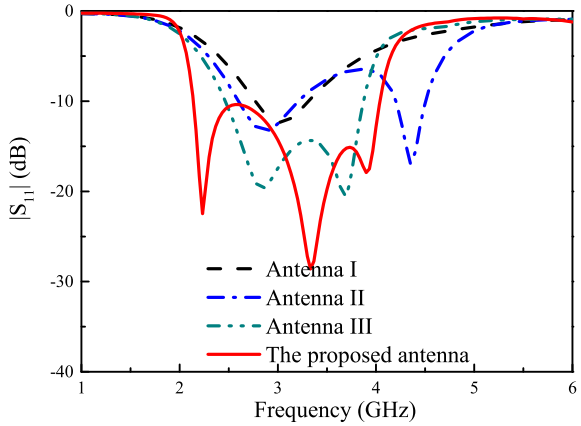

FIGURE 3. Simulated $|S_{11}|$-frequency curves of the reference and proposed antennas.

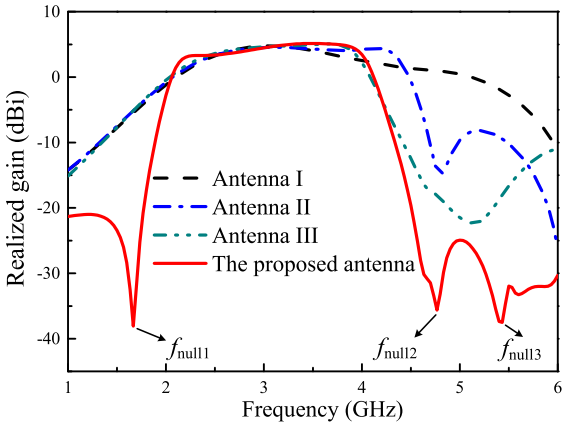

FIGURE 4. Simulated gain-frequency curves of the reference and proposed antennas.

Antenna I shows no filtering performance. Next, two parasitic patches are symmetrically loaded in the dumbbell-shaped slot to form Antenna II in Fig. 2. A new resonant frequency is introduced at 4.37 GHz for Antenna II, as shown by the blue line in Fig. 3. Fig. 5(a) illustrates that the current of Antenna II is mainly concentrated on two parasitic patches at 4.37 GHz, and the length of the parasitic patches (l_2) is half the waveguide wavelength of 4.37 GHz. Moreover, a gain null is generated at 4.78 GHz and the gain of Antenna II falls quickly in the high frequency band in Fig. 4. However, these two resonant frequencies of Antenna II are separated far apart. Then, Antenna III is formed by etching eight slot-stubs adjacent to the dumbbell-shaped slot based on Antenna II. The impedance matching is effectively improved and the impedance bandwidth is up to 44.5% (2.46 GHz - 3.87 GHz). Finally, the proposed filtering slot antenna is designed by adding a pair of SIR stubs on the feeding line. Fig. 3 shows that a new resonant frequency is generated in the lower band and the impedance bandwidth is furtherly increased to 61.5% (2.14 GHz - 4.04 GHz). This is because that the current is mainly concentrated on SIR stubs at 2.23 GHz in Fig. 5(b), and the length of it ($l_4 + l_5$) is the quarter waveguide wavelength of 2.23 GHz. Furthermore, the other two gain nulls in the low frequency band at 1.68 GHz (f_{null1}) and high frequency band at 5.44 GHz (f_{null3}) are achieved, as shown by the red line in Fig. 4. Therefore, the selectivity of the lower band is greatly improved and the out-of-band suppression level of the upper band is further enhanced. Meanwhile, the position of the gain null at 4.78 GHz (f_{null2}) remains unchanged. As a result, the proposed antenna has three gain nulls through the combined effect of parasitic patches and SIR stubs. Compared with the traditional dumbbell-shaped slot antenna, high frequency selectivity and out-of-band suppression level for the both band-edges are realized.

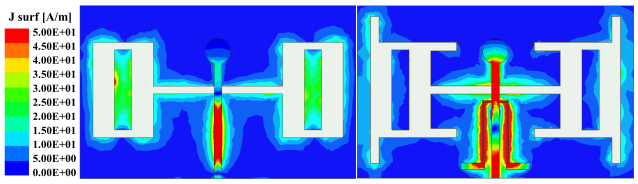

FIGURE 5. Simulated current distribution of (a) Antenna II at resonant frequency (4.37 GHz) and (b) the proposed antenna at resonant frequency (2.23 GHz).

To clarify the effect of the number of slot-stubs on the performance, the reflection coefficients under different numbers of slot-stubs are compared in Fig. 6. It can be found that as the number of slot-stubs is decreased from 8 to 0, the impedance matching in the higher band is degraded. In addition, when the slot-stubs are increased from 8 to 16, the bandwidth is significantly narrowed. Therefore, considering the impedance matching and bandwidth, eight slot-stubs adjacent to the dumbbell-shaped slot are the most suitable.

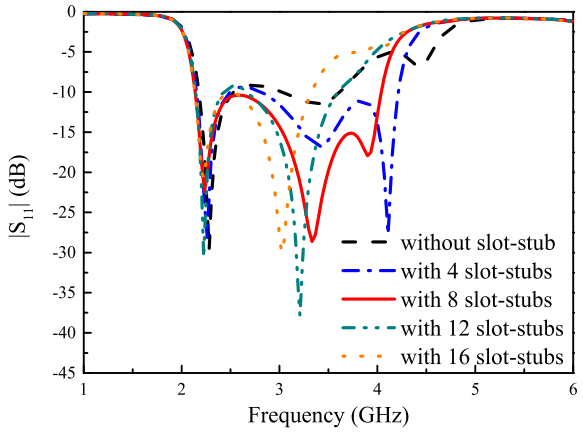

FIGURE 6. Simulated $|S_{11}|$-frequency curves of the proposed antenna without slot-stub, with 4 slot-stubs, with 8 slot-stubs, with 12 slot-stubs and 16 slot-stubs.

To further explain the principle of the generation of three gain nulls, Fig. 7 and Fig. 8 show the current distributions of the proposed antenna at them, respectively. Fig. 9 compares the radiation patterns of the proposed antenna at three gain nulls and the operating band. Different from the current distribution in the passband, there is the reverse current on both sides of the ground and on the parasitic patches at f_{null2} (4.78 GHz) in Fig. 7. The radiating fields in the far-field region generated by them are cancelled out. As can be observe from Fig. 9(c), the radiation pattern split into several lobes unlike that in Fig. 9(b) and a radiation null is generated in the z-axis direction, leading to the gain null in the gain curve at f_{null2} (4.78 GHz). Fig. 8 clarifies the two gain nulls (f_{null1} and f_{null3}) generated by SIR stubs. Fig. 8(b) shows that the dumbbell-shaped slot of the proposed antenna is completely excited at 3.5 GHz. However, Fig. 8(a) and (c) illustrate that most of the EM energy is reflected to the input port at f_{null1} (1.68 GHz) and f_{null3} (5.44 GHz). Because of the band-stop property of the SIR open stubs, there is no energy input

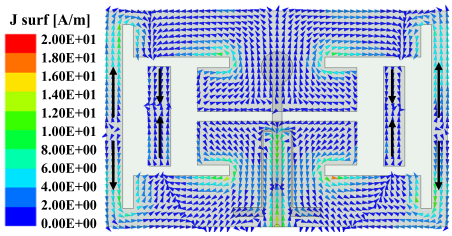

FIGURE 7. Simulated current distribution of the proposed antenna at f_{null2} (4.78 GHz).

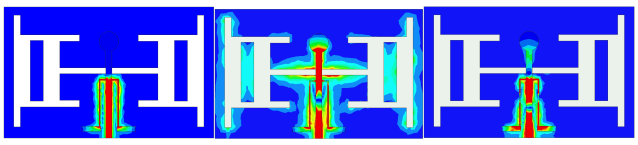

FIGURE 8. Simulated current distributions of the proposed antenna at (a) f_{null1} (1.68 GHz), (b) the operating band (3.5 GHz) and (c) f_{null3} (5.44 GHz).

into the dumbbell-shaped slot. It is demonstrated that the slot antenna is unexcited in Fig. 9(a) and (d), which results in two gain nulls at these two frequencies (f_{null1} and f_{null3}) in the gain curve.

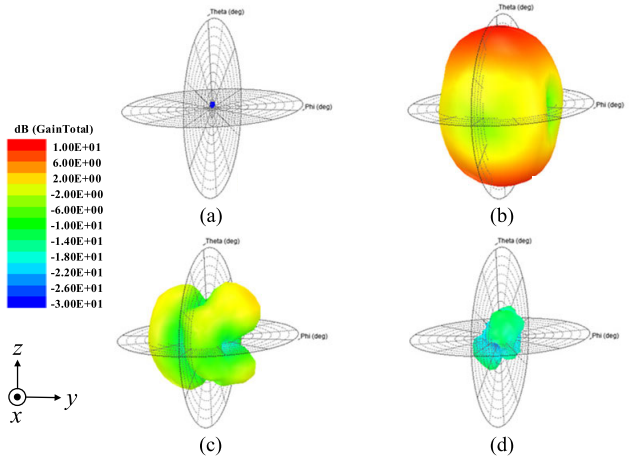

FIGURE 9. Radiation patterns of the proposed antenna at (a) f_{null1} (1.68 GHz), (b) the operating band (3.5 GHz), (c) f_{null2} (4.78 GHz), and (d) f_{null3} (5.44 GHz).

For the purpose of demonstrating the two gain nulls (f_{null1} and f_{null3}) generated by SIR stubs, the equivalent circuit of the proposed antenna is given in Fig. 10. The ABCD matrix and transmission coefficient of the equivalent circuit for it is calculated as follows:

$$\begin{bmatrix} A & B \\ C & D \end{bmatrix} = \begin{bmatrix} \cos\theta_1 & jZ_1 \cdot \sin\theta_1 \\ j\sin\theta_1/Z_1 & \cos\theta_1 \end{bmatrix} \begin{bmatrix} 1 & 0 \\ Y & 1 \end{bmatrix} \times \begin{bmatrix} \cos\theta_4 & jZ4 \cdot \sin\theta_4 \\ j\sin\theta_4/Z_4 & \cos\theta_4 \end{bmatrix} \quad (1)$$

$$Y = \frac{2}{Z_3} \cdot \frac{jZ_3 \cdot \tan\theta_2 + jZ_2 \cdot \tan\theta_3}{Z_2 - Z_3 \cdot \tan\theta_2 \cdot \tan\theta_3} \quad (2)$$

$$S_{21} = \frac{2}{A + B/Z_0 + C \cdot Z_0 + D} \quad (3)$$

The calculated S-parameter is shown in Fig. 11 and compared with the simulated realized gain. It can be seen that the frequencies of the two nulls (f_{null1} and f_{null3}) in the gain curve is in good agreement with the frequencies of the nulls calculated by the equivalent circuit. Thus, the frequency selectivity for the both band-edges can be significantly improved. In addition, it also means that the nulls generated by the SIR stubs and the parasitic patches are independent of each other and can be controlled individually.

C. PARAMETRIC STUDIES

To further illustrate the function of the parasitic patches and the SIR stubs on the filtering performance of the proposed antenna, the parametric analyses are presented in Fig. 12 and Fig. 13. Parameter l_2 is the length of parasitic patches. Fig. 12 shows the reflection coefficient and realized gain of the proposed antenna under different l_2. It can be observed that as l_2 increases from 17 mm to 20 mm, the impedance

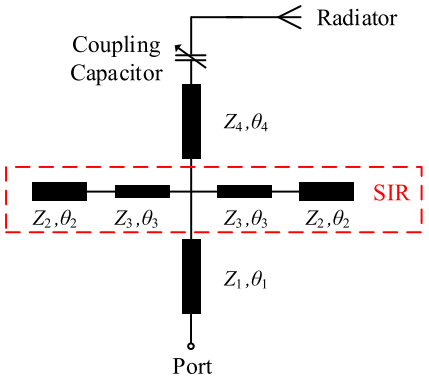

FIGURE 10. Equivalent circuit of the proposed antenna from input port to the radiator.

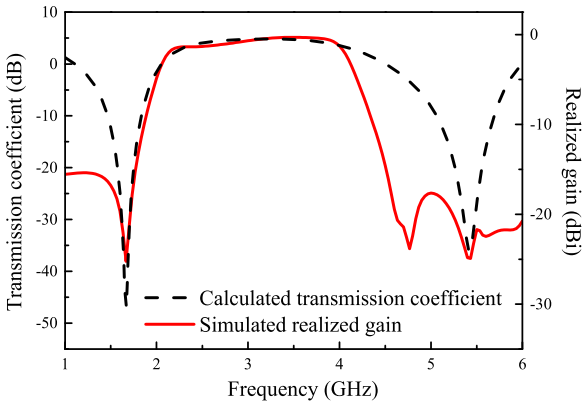

FIGURE 11. The comparison between the calculated transmission coefficient of the equivalent circuit and the simulated realized gain of the proposed antenna.

matching in the higher band is degraded. Moreover, the position of the null (f_{null2}) generated by the parasitic patches shifts toward the lower frequency band, and the other gain nulls are not influenced. Parameter l_4 is the partial length of SIR stubs. As shown in Fig. 13, the impedance matching in the lower band is affected by the change of l_4. Similarly, the gain nulls (f_{null1} and f_{null3}) introduced by the SIR stubs move to the lower frequency with the increase of the total length. It can be found that there is almost no impact on the position of the gain null (f_{null2}). The results of the parametric studies demonstrate that the positions of gain nulls can be adjusted independently.

III. MEASUREMENT OF ANTENNA

The prototype of the proposed wideband filtering dumbbell-shaped slot antenna has been manufactured and measured to verify the design. The photograph of the prototype is shown in Fig. 14, and the measured results by the using of Satimo near field measurement system are depicted in Fig. 15. The simulated impedance bandwidth of $|S_{11}| < -10$ dB is 61.5% (2.14 GHz - 4.04 GHz) and the simulated gain is stable at 4.5±0.5 dBi. The measured impedance bandwidth of it is 62.5% (2.2 GHz - 4.2 GHz), and the max measured gain

TABLE 1. Comparison between the proposed filtering slot antenna and reported paper.

Ref.	Filtering method	Frequency (GHz)	BW (%)	Size ($\lambda_0 \times \lambda_0$)	Gain (dBi)	Number of gain nulls	Frequency selectivity for the lower/upper band-edges (S_L/S_U)	Out-of-band suppression level for the lower/upper band (dB)
[4]	Open-loop resonator	2.4	14	0.36×0.25	2.4	none	1.29/1.86	25/23
[12]	Parasitic patch	3.6	9.9	0.61×0.61	7.5	two	-	4/5
[13]	Parasitic loop	3	56.6	0.61×0.51	5.4	one	0.4/0.2	20/13
[14]	Parasitic strip	2.3	30.4	0.54×0.38	5.7	two	0.47/0.27	21/19
[23]	Multimode resonator	5.2	25	0.62×0.5	3	one	1.15/0.38	20/17
[24]	Multimode resonator	5.2	46.1	1.13×0.87	5	two	0.21/-	23/10
This work	Parasitic patch +SIR stub	3.1	61.5	0.66×0.41	4.5	three	0.19/0.24	26/30

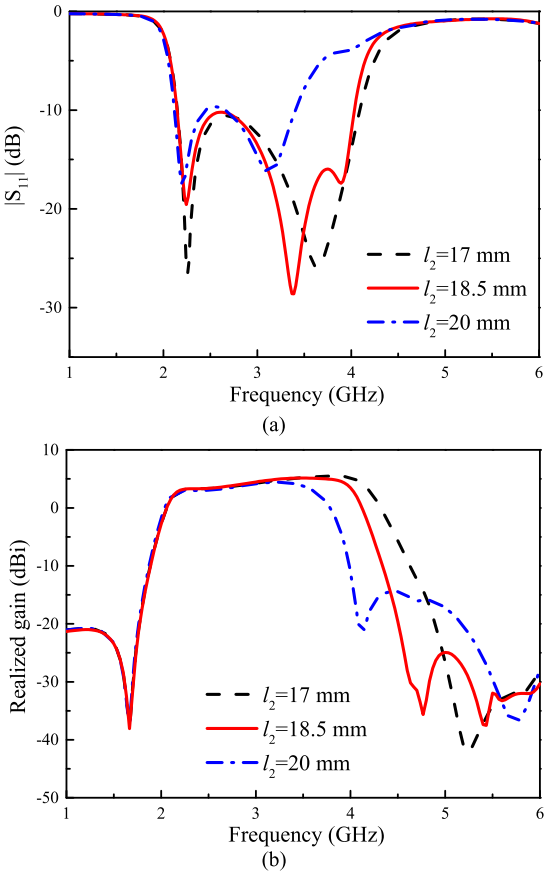

FIGURE 12. Simulated (a) reflection coefficient and (b) realized gain of the proposed antenna under different l_2.

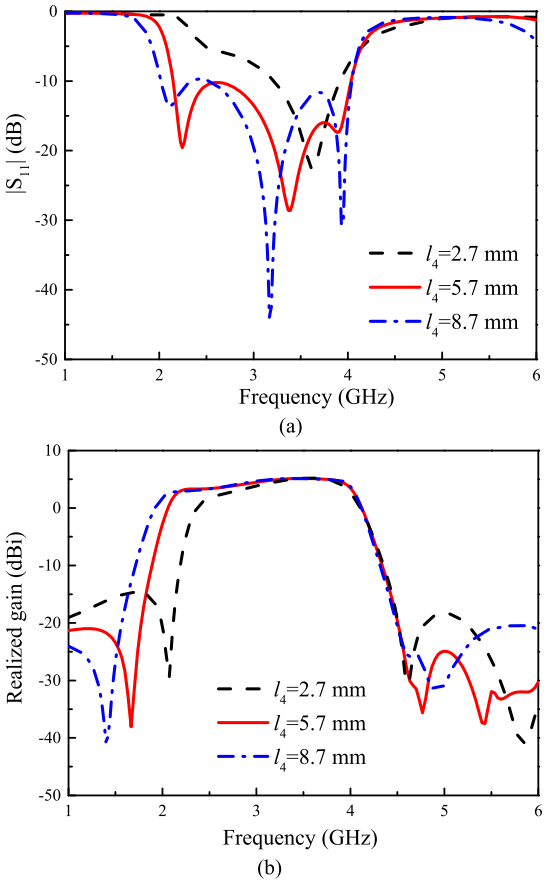

FIGURE 13. Simulated (a) reflection coefficient and (b) realized gain of the proposed antenna under different l_4.

is 5 dBi. The measured results agree well with the simulated results.

Fig. 16 shows the measured total efficiency in the passband is above 80%. It also exhibits that the proposed antenna has the high selectivity of efficiency. It can be observed that the measured curves shift a little towards the high frequency band. By analyzing the influence of the dielectric constant on the simulated results, the simulated results with dielectric constant of 4.0 are more coincident with the measured results. Therefore, the deviation between simulated and measured results is mainly due to the error of dielectric constant of substrate. The limitation on the accuracy of manufacturing and measuring also affect the measured results. The simulated and measured normalized radiation patterns at the three resonances of 2.23 GHz, 3.34 GHz and 3.91 GHz are shown in Fig. 17, respectively.

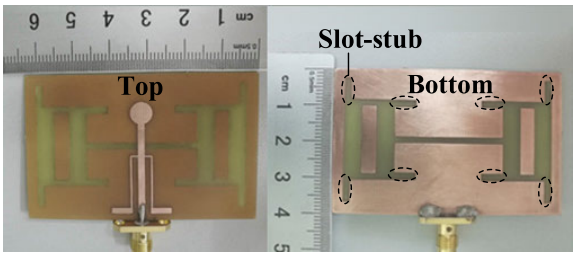

FIGURE 14. Photograph of the proposed filtering slot antenna.

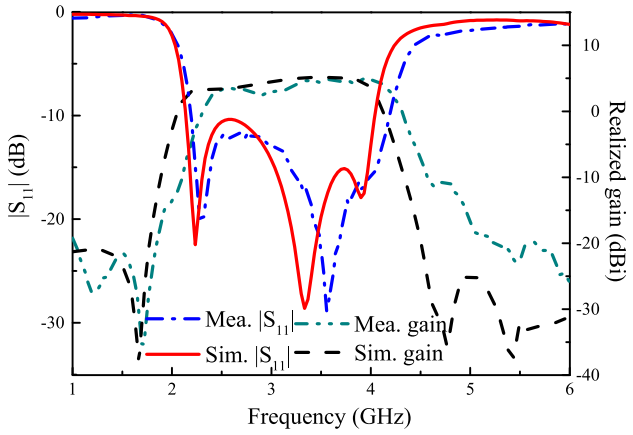

FIGURE 15. Simulated and measured reflection coefficient and realized gain of the proposed filtering slot antenna.

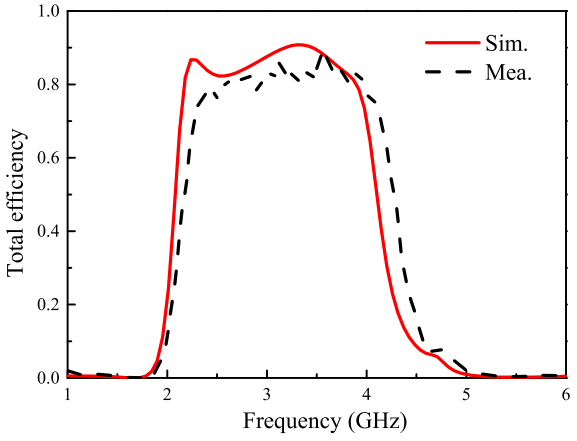

FIGURE 16. Simulated and measured total efficiency of the proposed filtering slot antenna.

The comparison of the simulated performance between the proposed filtering antenna and reported works is presented in Table 1. λ_0 is the wavelength of the center frequency in free space. The frequency selectivity for the lower (S_L) and upper (S_U) band-edges can be defined as follows [26]:

$$S_L = \frac{f^1_{10L} - f^2_{\Delta 20L}}{f^1_{10U} - f^1_{10L}}, \quad S_U = \frac{f^2_{\Delta 20U} - f^1_{10U}}{f^1_{10U} - f^1_{10L}} \tag{4}$$

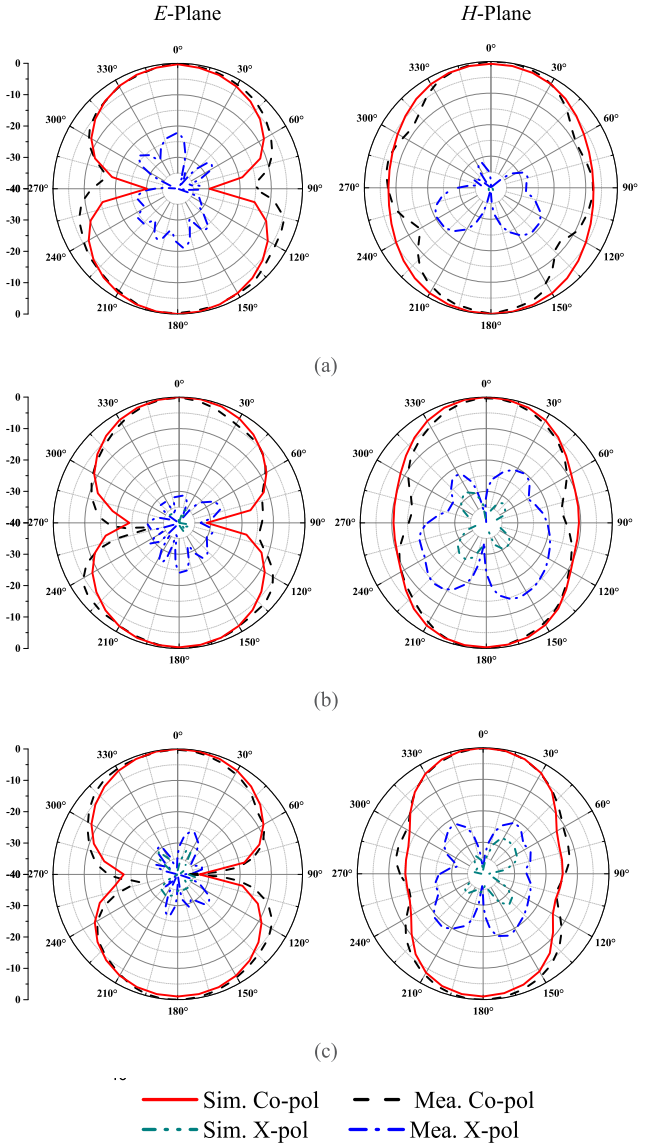

FIGURE 17. Simulated and measured normalized radiation patterns in the two main planes at three resonances. (a)2.23 GHz, (b)3.34 GHz, and (c)3.91 GHz.

where f^1_{10L} and f^1_{10U} represent the frequencies of the lower and upper band-edges with $|S_{11}| = -10$dB. $f^2_{\Delta 20L}$ and $f^2_{\Delta 20U}$ are the frequencies corresponding to the upper and lower band-edges when the gain of the center frequency drops by 20dB. Smaller S_L or S_U means higher frequency selectivity. After comparison, it can be found that the designs in [4] and [12] suffer limited impedance bandwidth. Although the filtering performance is realized in [13] and [14], the frequency selectivity is not high for the both band-edges. Due to the integration of multimode resonator, the gain of the filtering slot antenna is low in [23] and the occupied size is relatively large in [24]. By the combination of parasitic patches and SIR stubs, the proposed antenna has a wider bandwidth, higher frequency selectivity, and better out-of-band suppression level.

IV. CONCLUSION

A novel wideband filtering dumbbell-shaped slot antenna with improved frequency selectivity for both band-edges is proposed. The bandwidth of it can be greatly broadened by loading parasitic patches and a pair of SIR stubs. Three gain nulls can also be obtained at 1.68 GHz, 4.78 GHz and 5.44 GHz, respectively. Due to the generation of the gain nulls, the antenna gain flatness and frequency selectivity can be effectively enhanced. Moreover, the gain nulls can be controlled independently by changing the length of parasitic patches or SIR stubs. The measured bandwidth of $|S_{11}| < -10$ dB is 62.5% (2.2 GHz - 4.2 GHz), and the gain is steady within the passband. The antenna can be applied in ISM Band (2.45 GHz), Wi-MAX (2.5 GHz - 2.69 GHz and 3.2 GHz - 3.8 GHz) and 5G (3.3 GHz - 3.6 GHz) wireless communication system.

REFERENCES

[1] C.-Y. Hsieh, C.-H. Wu, and T.-G. Ma, "A compact dual-band filtering patch antenna using step impedance resonators," *IEEE Antennas Wireless Propag. Lett.*, vol. 14, pp. 1056–1059, Jan. 2015.

[2] Y. Yao, Z.-H. Tu, and Z. Gan, "A tri-band monopole filtering antenna using multimode resonators," *Microw. Opt. Technol. Lett.*, vol. 59, no. 8, pp. 1908–1913, Aug. 2017.

[3] C. X. Mao, S. Gao, Y. Wang, B. Sanz-Izquierdo, Z. Wang, F. Qin, Q. X. Chu, J. Li, G. Wei, and J. Xu, "Dual-band patch antenna with filtering performance and harmonic suppression," *IEEE Trans. Antennas Propag.*, vol. 64, no. 9, pp. 4074–4077, Sep. 2016.

[4] W.-J. Wu, Y.-Z. Yin, S.-L. Zuo, Z.-Y. Zhang, and J.-J. Xie, "A new compact filter-antenna for modern wireless communication systems," *IEEE Antennas Wireless Propag. Lett.*, vol. 10, pp. 1131–1134, 2011.

[5] J.-F. Qian, F.-C. Chen, Y.-H. Ding, H.-T. Hu, and Q.-X. Chu, "A wide stopband filtering patch antenna and its application in MIMO system," *IEEE Trans. Antennas Propag.*, vol. 67, no. 1, pp. 654–658, Jan. 2019.

[6] K.-D. Xu, H. Xu, and Y. Liu, "Low-profile filtering end-fire antenna integrated with compact bandstop filtering element for high selectivity," *IEEE Access*, vol. 7, pp. 8398–8403, 2019.

[7] C.-H. Wu, C.-H. Wang, S.-Y. Chen, and C. Hsiung Chen, "Balanced-to-unbalanced bandpass filters and the antenna application," *IEEE Trans. Microw. Theory Techn.*, vol. 56, no. 11, pp. 2474–2482, Nov. 2008.

[8] T. L. Wu, Y. M. Pan, P. F. Hu, and S. Y. Zheng, "Design of a low profile and compact omnidirectional filtering patch antenna," *IEEE Access*, vol. 5, pp. 1083–1089, 2017.

[9] C.-K. Lin and S.-J. Chung, "A compact filtering microstrip antenna with quasi-elliptic broadside antenna gain response," *IEEE Antennas Wireless Propag. Lett.*, vol. 10, pp. 381–384, Apr. 2011.

[10] J. Y. Jin, S. Liao, and Q. Xue, "Design of filtering-radiating patch antennas with tunable radiation nulls for high selectivity," *IEEE Trans. Antennas Propag.*, vol. 66, no. 4, pp. 2125–2130, Apr. 2018.

[11] X. Zhang, Q.-S. Wu, L. Zhu, G.-L. Huang, and T. Yuan, "Resonator-fed wideband and high-gain patch antenna with enhanced selectivity and reduced cross-polarization," *IEEE Access*, vol. 7, pp. 49918–49927, 2019.

[12] W. Wang, J. Ran, N. Hu, W. Xie, Y. Wu, and A. Kishk, "A novel differential filtering patch antenna with high selectivity," *Int. J. RF Microw. Comput.-Aided Eng.*, vol. 29, no. 10, Oct. 2019, Art. no. e21880.

[13] J. Wu, Z. Zhao, Z. Nie, and Q.-H. Liu, "A printed unidirectional antenna with improved upper band-edge selectivity using a parasitic loop," *IEEE Trans. Antennas Propag.*, vol. 63, no. 4, pp. 1832–1837, Apr. 2015.

[14] G. Liu, Y. M. Pan, T. L. Wu, and P. F. Hu, "A compact planar quasi-Yagi antenna with bandpass filtering response," *IEEE Access*, vol. 7, pp. 67856–67862, 2019.

[15] P. F. Hu, Y. M. Pan, X. Y. Zhang, and S. Y. Zheng, "Broadband filtering dielectric resonator antenna with wide stopband," *IEEE Trans. Antennas Propag.*, vol. 65, no. 4, pp. 2079–2084, Apr. 2017.

[16] B. J. Xiang, S. Y. Zheng, Y. M. Pan, and Y. X. Li, "Wideband circularly polarized dielectric resonator antenna with bandpass filtering and wide harmonics suppression response," *IEEE Trans. Antennas Propag.*, vol. 65, no. 4, pp. 2096–2101, Apr. 2017.

[17] Y. M. Pan, P. F. Hu, X. Y. Zhang, and S. Y. Zheng, "A low-profile high-gain and wideband filtering antenna with metasurface," *IEEE Trans. Antennas Propag.*, vol. 64, no. 5, pp. 2010–2016, May 2016.

[18] W. Yang, S. Chen, Q. Xue, W. Che, G. Shen, and W. Feng, "Novel filtering method based on metasurface antenna and its application for wideband high-gain filtering antenna with low profile," *IEEE Trans. Antennas Propag.*, vol. 67, no. 3, pp. 1535–1544, Mar. 2019.

[19] G. Zhang, L. Ge, J. Wang, and J. Yang, "Design of a 3-D integrated wideband filtering magneto-electric dipole antenna," *IEEE Access*, vol. 7, pp. 4735–4740, 2019.

[20] C.-H. Lee, S.-Y. Chen, and P. Hsu, "Isosceles triangular slot antenna for broadband dual polarization applications," *IEEE Trans. Antennas Propag.*, vol. 57, no. 10, pp. 3347–3351, Oct. 2009.

[21] N. Behdad and K. Sarabandi, "A wide-band slot antenna design employing a fictitious short circuit concept," *IEEE Trans. Antennas Propag.*, vol. 53, no. 1, pp. 475–482, Jan. 2005.

[22] X. Bi, G.-L. Huang, X. Zhang, and T. Yuan, "Design of wideband and high-gain slotline antenna using multi-mode radiator," *IEEE Access*, vol. 7, pp. 54252–54260, 2019.

[23] H.-W. Deng, T. Xu, and F. Liu, "Broadband pattern-reconfigurable filtering microstrip antenna with quasi-yagi structure," *IEEE Antennas Wireless Propag. Lett.*, vol. 17, no. 7, pp. 1127–1131, Jul. 2018.

[24] H.-T. Hu, F.-C. Chen, and Q.-X. Chu, "Novel broadband filtering slotline antennas excited by multimode resonators," *IEEE Antennas Wireless Propag. Lett.*, vol. 16, pp. 489–492, Jun. 2017.

[25] M. Leib, M. Frei, and W. Menzel, "A microstrip-fed ultra-wideband slot antenna," in *Proc. IEEE Antennas Propag. Soc. Int. Symp.*, Jun. 2009, pp. 1–4.

[26] K. Xu, J. Shi, X. Qing, and Z. N. Chen, "A substrate integrated cavity backed filtering slot antenna stacked with a patch for frequency selectivity enhancement," *IEEE Antennas Wireless Propag. Lett.*, vol. 17, no. 10, pp. 1910–1914, Oct. 2018.

NA NIE was born in Yichun, Jiangxi, China. She received the B.S. degree in communication engineering from Yanshan University, Qinhuangdao, China, in 2017. She is currently pursuing the Ph.D. degree with the South China University of Technology, Guangzhou. Her current research interests include filtering antennas, millimeter-wave antennas, and dual-band large-frequency-ratio antennas.

ZHI-HONG TU (Member, IEEE) received the Ph.D. degree from the South China University of Technology, Guangzhou, China, in 2007. Since 2008, she has been with the School of Electronic and Information Engineering, South China University of Technology, where she is currently a Full Professor. From 2011 to 2012, she was a Research Staff with the School of Electrical and Electronic Engineering, Nanyang Technological University, Singapore. Her current research interests include microwave and millimeter-wave antennas, array and circuit, synthesis theory and design of microwave filters, and associated RF modules.